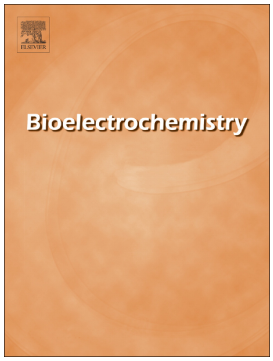

Electrochemical DNA biosensor for detection of DNA damage induced by hydroxyl radicals

Andrea Hájková, Jiří Barek, Vlastimil Vyskočil

PII: S1567-5394(17)30100-7
DOI: doi: 10.1016/j.bioelechem.2017.02.003
Reference: BIOJEC 6995

To appear in: *Bioelectrochemistry*

Received date: 18 September 2016
Revised date: 23 February 2017
Accepted date: 26 February 2017

Please cite this article as: Andrea Hájková, Jiří Barek, Vlastimil Vyskočil , Electrochemical DNA biosensor for detection of DNA damage induced by hydroxyl radicals. The address for the corresponding author was captured as affiliation for all authors. Please check if appropriate. Biojec(2017), doi: 10.1016/j.bioelechem.2017.02.003

Electrochemical DNA biosensor for detection of DNA damage induced by hydroxyl radicals

Andrea Hájková*, Jiří Barek, and Vlastimil Vyskočil*

Charles University, Faculty of Science, Department of Analytical Chemistry, UNESCO Laboratory of Environmental Electrochemistry, Hlavova 2030/8, 128 43 Prague 2, Czech Republic

*Corresponding author.
E-mail addresses: andrea.hajkova@natur.cuni.cz (A. Hájková), vlastimil.vyskocil@natur.cuni.cz (V. Vyskočil).

Abstract

A simple electrochemical DNA biosensor based on a glassy carbon electrode (GCE) was prepared by adsorbing double-stranded DNA (dsDNA) onto the GCE surface and subsequently used for the detection of dsDNA damage induced by hydroxyl radicals. Investigation of the mutual interaction between hydroxyl radicals and dsDNA was conducted using a combination of several electrochemical detection techniques: square-wave voltammetry for direct monitoring the oxidation of dsDNA bases, and cyclic voltammetry and electrochemical impedance spectroscopy as indirect electrochemical methods making use of the redox-active indicator $[Fe(CN)_6]^{4-/3-}$. Hydroxyl radicals were generated electrochemically on the surface of a boron-doped diamond electrode and chemically (via the Fenton's reaction or the auto-oxidation of Fe(II)). The extent of dsDNA damage by electrochemically generated hydroxyl radicals depended on the current density applied to the generating electrode: by applying 5, 10, and 50 mA cm^{-2}, selected relative biosensor responses decreased after 3 min incubation from 100% to 38%, 27%, and 3%, respectively. Chemically generated hydroxyl radicals caused less pronounced dsDNA damage, and their damaging activity depended on the form of Fe(II) ions: decreases to 49% (Fenton's reaction; Fe(II) complexed with EDTA) and 33% (auto-oxidation of Fe(II); Fe(II) complexed with dsDNA) were observed after 10 min incubation.

Keywords: Electrochemical DNA biosensor; Glassy carbon electrode; Hydroxyl radicals; Boron-doped diamond electrode; Fenton's reaction; Auto-oxidation

1. Introduction

Oxidation of tissues (oxidative stress) is connected with the production of reactive oxygen species (ROS) [1], which can be main source of damage to cell structures, including lipids and membranes, proteins and nucleic acids [1-3]. The ROS, such as superoxide radical ($O_2^{\bullet -}$), hydroxyl radical ($OH^{\bullet}$), hydrogen peroxide (H_2O_2), *etc.*, can be generated inside cells as products of metabolism [3-5]. Their normal concentration level in organisms has important physiological effects on transcription factors and cell proliferation and differentiation [4,6]. However, when the organisms are suffering from harmful environmental stress, such as irradiation by UV light, X-rays, or gamma rays, intoxication by heavy metals or organic pollutants, excessive drinking of alcohol, *etc.*, or when the antioxidant system is in disorder [2,4,7], the ROS levels can increase dramatically – oxidative stress then occurs [4,7]. Oxidative stress that occurs in living systems can cause cellular death, aging, and many diseases such as arteriosclerosis [4,8], ischemia/reperfusion injury, hepatitis, Parkinson's and Alzheimer's diseases, rheumatoid arthritis, brain ischemia, stroke, and carcinogenesis [6,9-11].

Hydroxyl radicals are one of the most reactive radical species that induce lesions in DNA [7] by abstracting hydrogen atoms or by direct adduct formation with nucleobases [12]. These radicals oxidize the DNA bases and deoxyribose, which leads to the release of the bases and to the interruption of the phosphodiester bonds [8]. This results in nucleotide oxidation in DNA, which may generate replication errors and subsequent misleading protein synthesis [13]. A variety of modifications at the DNA level, including base and sugar lesions, strand breaks, DNA–protein cross-link, and base-free sites, can be detected [7,8,13]; for instance, disruption of the electroactive sites in some bases may lead to a loss of their intrinsic electroactivity [3].

Studies of DNA damage are of special importance because DNA is the repository of genetic information [13]. Various methods have helped to characterize the nature of the interaction of hydroxyl radicals with DNA, but they have provided conflicting results [5]. Consequently, consensus and clarification of this interaction is still needed. In recent years, electrochemical DNA biosensors for the detection of DNA damage induced by ROS have become important tools in evaluation of oxidative stress to DNA [3,4]. In paper [3], two electrochemical DNA biosensors (the first one composed of a commercially available screen-printed carbon electrode (SPCE) and low molecular weight double-stranded DNA (dsDNA); the second one composed of a SPCE, a composite of carboxylated single-walled carbon nanotubes and chitosan, and low molecular weight dsDNA) were developed and successfully applied for this purpose. However, their preparation is time-consuming (DNA is dropped onto

the bare SPCE or the composite-modified SPCE and left to evaporate to dryness for several hours) and rather costly (a lot of SPCEs are needed since a new disposable SPCE is required for each application of these biosensors, and expensive derivatized carbon nanotubes are also required in the case of the nanostructured version).

In the presented study, a simple electrochemical DNA biosensor based on a glassy carbon electrode (GCE) and low molecular weight dsDNA (firstly introduced in our recent paper [14] where it was used for the investigation of supramolecular interactions between dsDNA and genotoxic 2-aminofluoren-9-one) is newly employed for the detection of dsDNA damage induced by hydroxyl radicals. Contrary to the above-mentioned dsDNA/SPCE biosensors [3], the preparation of this dsDNA/GCE biosensor requires only one substrate electrode which can be used repeatedly. Moreover, dsDNA is adsorbed electrostatically on the GCE surface [14], and the whole DNA biosensor preparation thus takes no more than 5 min in comparison to very time-consuming procedures making use of the air-drying a DNA solution on the electrode surface [15].

A comprehensive electrochemical biosensing approach in the detection of DNA damage (introduced by Labuda *et al.* [3,16] and further developed and improved in our recent paper [14] and in the presented study) represents a novel model for *in vitro* classification of potentially genotoxic chemicals (ROS, environmental pollutants, pesticides, conventional or newly synthesized drugs, *etc.*). It is based on a set of criteria that determine whether and under which conditions the investigated agent causes damage to DNA. Combination of several electrochemical detection techniques is used in this approach [3,14,16]: (i) square-wave voltammetry (SWV) for direct monitoring of changes in the electrochemical behavior of dsDNA bases, and (ii) cyclic voltammetry (CV) and electrochemical impedance spectroscopy (EIS) as indirect electrochemical methods making use of the redox-active indicator $[Fe(CN)_6]^{4-/3-}$.

The aim of the presented work was to investigate the mutual interaction between hydroxyl radicals and dsDNA and to detect oxidative dsDNA damage using the dsDNA/GCE biosensor in combination with the above-mentioned comprehensive electrochemical biosensing approach. Contrary to the paper [3], which describes the generation of hydroxyl radicals by UV light and by the Fenton's like reaction involving Cu(II), three other sources of hydroxyl radicals are used here: (i) electrochemical generation of hydroxyl radicals on the surface of a boron-doped diamond electrode (BDDE) (used for the first time in the arrangement where the DNA biosensor surface is placed close to the BDDE surface, as shown in Fig. 1; in other cases, DNA is adsorbed on the BDDE surface, and oxidative damage by

electrochemically generated hydroxyl radicals is detected directly on the BDDE [5]), and chemical generation of hydroxyl radicals (ii) via the Fenton's reaction (of a newly optimized composition) and (iii) via the auto-oxidation of Fe(II) (whose effects on dsDNA were, to the best of our knowledge, investigated electrochemically for the first time).

1.1 Electrochemical generation of hydroxyl radicals on the BDDE

BDDEs have been extensively studied in recent years, from the point of view of their applications and their physical, chemical, and electronic properties [17]. The BDDE exhibits a high chemical and electrochemical stability [18]. It possesses technologically important characteristics such as chemically inert surface with low adsorption properties, high hardness, remarkable corrosion stability, extremely wide potential window in both aqueous and non-aqueous media [5,17,19,20], high thermal conductivity, and possible application of high current densities [17,20]. The BDDEs are used to produce hydroxyl radicals which are able to destroy non-selectively most of organic and organometallic contaminants, giving dehydrogenated or hydroxylated derivatives, until their complete mineralization, *i.e.*, their conversion into CO_2, water, and inorganic ions [18].

Hydroxyl radicals are electrochemically generated on the BDDE surface from water discharge at high potentials in acidic, neutral, or alkaline media [5,18]. The electrochemical anodic oxidation process is described by the following equation [21]:

$$BDDE + H_2O \rightarrow BDDE(OH^{\bullet}) + H^+ + e^-$$

1.2 Chemical generation of hydroxyl radicals using the Fenton's reaction

In living systems, many of the hydroxyl radicals are generated from the metal ion-dependent breakdown of H_2O_2 [13] which is arising from peroxisomes as well as during the reduction of molecular oxygen [12]. In the presence of Fe(II) or Cu(II) ions, H_2O_2 is converted into the hydroxyl radical by the Fenton's reaction or the Fenton's like reaction, respectively [13,22]. The Fenton's reagents are composed of Fe(II) ions and H_2O_2, and the formation process of hydroxyl radicals in the Fenton's reaction is as follows [7,16]:

$$Fe(II) + H_2O_2 \rightarrow Fe(III) + OH^{\bullet} + OH^-$$

In this reaction, Fe(II) is oxidized to Fe(III) by H_2O_2 and free hydroxyl radicals are produced [6]. The reaction time between hydroxyl radicals and a target molecule depends on the half-life time of the generated free radicals. It was found that for the concentrations of H_2O_2 or Fe(II) < 0.1 mmol L^{-1}, the Fenton's reaction might be completed within 1 s [13]. Hydroxyl radicals produced through the Fenton's reaction play a major role in DNA oxidative

damage [22]. Ethylenediaminetetraacetic acid (EDTA) is often included in the Fenton's reaction mixture as a chelating agent to increase the solubility of Fe(II) ions [7,13]. The presence of an Fe(II)–EDTA complex inhibits or stimulates oxidation reactions, depending on the molar ratio of Fe:EDTA, pH, or even on the method of preparation of the complex [6].

1.3 Chemical generation of hydroxyl radicals using auto-oxidation of Fe(II)

Iron (in a form of its species) is an essential nutriment for normal cellular functions. It is useful for function in cytochromes, oxygen-binding molecules, and many enzymes [6,22]. DNA binds to various metal ions because of its polyanionic nature and is, therefore, especially prone to iron-dependent, site-specific oxidative damage [6]. Moreover, when a complexing agent (EDTA) is not used in the Fenton's reaction mixture, free Fe(II) ions are capable of binding to DNA (forming an Fe(II)–DNA complex) [23]. Iron species firstly binds to DNA, and, then, Fe(II) is oxidized to Fe(III) [24].

The auto-oxidation of Fe(II) with dissolved oxygen molecules is another process that can produce ROS. The mechanism of the ROS production by the auto-oxidation of Fe(II) is still under debate. The generation of superoxide radicals arises from the reaction between Fe(II) and molecular oxygen. Subsequently, the superoxide radicals are dismutated to H_2O_2 which can serve as the precursor of the hydroxyl radical in the Fenton's reaction. These reactions can be described by following equations [16,25]:

$$Fe(II) + O_2 \leftrightarrow Fe(III) + O_2^{\bullet -}$$

$$2O_2^{\bullet -} + 2H^+ \leftrightarrow O_2 + H_2O_2$$

$$Fe(II) + H_2O_2 \rightarrow Fe(III) + OH^{\bullet} + OH^-$$

2. Experimental

2.1. Reagents

Low molecular weight salmon sperm double-stranded DNA (dsDNA; Product No. 31149, Sigma–Aldrich, Saint Louis, MO, USA) was stored in the fridge at 4°C, and a stock solution of dsDNA (γ = 10 mg mL^{-1}) in the 0.1 mol L^{-1} phosphate buffer of pH 6.7 (PB) was stored in the freezer at –18°C. Lower concentrations of dsDNA were prepared by the dilution of the dsDNA stock solution with the PB. PB was prepared by dissolving the calculated amount of disodium hydrogen phosphate dodecahydrate and sodium dihydrogen phosphate monohydrate. The equimolar mixture (c = 1 mmol L^{-1}) of potassium ferricyanide and potassium ferrocyanide ($[Fe(CN)_6]^{4-/3-}$) was prepared in the PB. A 0.1 mol L^{-1} acetate buffer of pH 4.7 (sodium acetate trihydrate in the solution of acetic acid), hydrogen peroxide

solution (30%, w/w) in water, Fe(II) sulphate heptahydrate ($FeSO_4 \cdot 7\ H_2O$), and EDTA were used for the Fenton's reaction (all of p.a. purity, Lach-Ner, Neratovice, Czech Republic). All the solutions were stored in glass vessels in the dark at laboratory temperature, except the dsDNA concentrated stock solution mentioned above.

2.2. Electrochemical apparatus

Electrochemical measurements were performed with a μAutolab III/FRA2 potentiostat driven by a GPES 4.9 software for voltammetric measurements and by a FRA 4.9 software for electrochemical impedance spectroscopic measurements (all Eco Chemie, Utrecht, Netherlands). For the preparation of the dsDNA/GCE biosensor, an Eco-Tribo electrochemical analyzer driven by a Polar Pro 5.1 software (both Polaro-Sensors, Prague, Czech Republic) was used. The measurements were carried out in a three-electrode system – a platinum wire auxiliary electrode (type Pt 1+L(P)), a silver/silver chloride reference electrode (type 10-20+, 3 mol L^{-1} KCl) (both from Elektrochemické detektory, Turnov, Czech Republic), and a glassy carbon electrode (GCE; a disc diameter of 2.0 mm, Eco Chemie, Utrecht, Netherlands) as working electrode. The GCE was cleaned mechanically by wiping with a microfiber cloth. It was polished using an aluminum oxide suspense (a particle size of 0.5 μm, Elektrochemické detektory, Turnov, Czech Republic), which was indispensable for effective immobilization of dsDNA. The boron-doped diamond electrode (BDDE) for the generation of hydroxyl radicals was prepared by chemical vapor deposition, using a $CH_4/H_2/B_2H_6$ source gas mixture consisting of 1% of carbon with 10 ppm of B_2H_6 added for boron doping (Institute of Physics of the Czech Academy of Sciences, Prague, Czech Republic). The system pressure was 18.67 kPa, and the substrate temperature was 800°C. The diamond film was deposited on silicon plates (1 × 1 cm), and its thickness was 1 μm.

2.3. Electrochemical procedures

Unless stated otherwise, all experiments consisted of four general steps: (i) mechanical cleaning and/or electrochemical activation of the GCE surface, (ii) electrochemical adsorption of dsDNA on the GCE, (iii) immersion of the prepared dsDNA/GCE biosensor into the incubation solution with hydroxyl radicals (or into the blank solution, *i.e.*, the incubation solution where no hydroxyl radicals were generated), and (iv) detection and evaluation of dsDNA damage induced by hydroxyl radicals: direct electrochemical method based on the oxidation of dsDNA bases (utilizing square-wave voltammetry (SWV)) and indirect electrochemical methods making use of the redox-active indicator $[Fe(CN)_6]^{4-/3-}$ (utilizing

cyclic voltammetry (CV) and electrochemical impedance spectroscopy (EIS)). DNA was adsorbed using an electrochemical adsorptive accumulation step with chosen adsorption potential and adsorption time (see Section 3.1). For the generation of hydroxyl radicals, a fresh Fenton's reaction mixture was always prepared for each measurement. Hydroxyl radicals were generated by the galvanostatic electrolysis on the BDDE, too. Each SWV or CV/EIS (CV followed by EIS) biosensor response was registered at the newly prepared dsDNA/GCE biosensor.

2.4. Parameters of methods

In CV, a scan rate of 0.05 V s^{-1} was used. For SWV, a scan rate of 3 V s^{-1}, a pulse amplitude of 0.05 V, a step potential 0.015 V, and a frequency of 200 Hz were applied. In EIS, a frequency range of 0.1–5000 Hz (51 frequency steps), a potential amplitude of 0.01 V, and a polarization potential of 0.225 V were used.

At the SWV measurements of the heights of the guanosine and adenosine peaks (the peak current was evaluated against the baseline), the surviving portion of dsDNA (*i.e.*, a relative biosensor response to dsDNA damage (S_{rel})) was calculated using the equation: S_{rel} (%) = (S_1/S_0)×100, where S_0 and S_1 are signals recorded before and after the interaction of dsDNA with hydroxyl radicals, respectively [14]. On the other hand, at the CV (the peak currents of the anodic ($I_{p,a}$) and cathodic ($I_{p,c}$) peaks of $[Fe(CN)_6]^{4-/3-}$ were evaluated from the extrapolated linear portion of the voltammogram before the onset of the peak) and EIS (the Nyquist plots were fitted using an R1(Q1[R2W1]) equivalent circuit, and the charge transfer resistance (R_{CT}) was evaluated) experiments, a relative biosensor response to dsDNA damage (ΔS_{rel}) was calculated using the equation: ΔS_{rel} (%) = [(S_1–S)/(S_0–S)]×100, where S_0 and S_1 are signals recorded before and after the interaction of dsDNA with hydroxyl radicals, respectively, and S is a signal recorded at the electrode without a DNA layer [14], *i.e.*, at the bare GCE. Each relative biosensor response was corrected to a biosensor blank (no hydroxyl radicals were generated in the incubation solution).

3. Results and discussion

3.1. Preparation of the dsDNA/GCE biosensor

The electrochemical DNA biosensor based on the GCE (dsDNA/GCE biosensor) was prepared by the adsorption of dsDNA on the GCE. The GCE surface was cleaned mechanically (polished using the aluminum oxide suspense – particle size of 0.5 μm).

Optimum parameters of the dsDNA adsorption were searched for: the concentration of dsDNA (γ_{ads}), the adsorption potential (E_{ads}), and the adsorption time (t_{ads}).

SWV was used as direct electrochemical method for monitoring the oxidation of dsDNA bases. For the preparation of the dsDNA/GCE biosensor to be applied with SWV, optimum adsorption parameters were taken from [14]: γ_{ads} of 0.1 mg mL^{-1} of dsDNA in the PB, E_{ads} of 0.5 V, t_{ads} of 0.5 min, and stirring the solution during the accumulation. After that, the prepared dsDNA/GCE biosensor was washed in the PB for 5 s, and the recordings of SWV were performed in the PB.

For application of indirect electrochemical methods making use of the redox-active indicator $[Fe(CN)_6]^{4-/3-}$ (CV and EIS), the parameters of the dsDNA adsorption were newly optimized. Firstly, the bare GCE was electrochemically cleaned using consecutive application of two activation potentials (E_{act}) for given activation times (t_{act}) in stirred solution of $[Fe(CN)_6]^{4-/3-}$ in the PB: $E_{act,1}$ of 1.7 V, $t_{act,1}$ of 1 min, and $E_{act,2}$ of –0.5 V, $t_{act,2}$ of 1 min. Afterwards, dsDNA was adsorbed on the GCE under following optimum conditions: γ_{ads} of 10 mg mL^{-1} of dsDNA in the PB, E_{ads} of 0.5 V, t_{ads} of 3 min, and stirring the solution during the accumulation. After that, the prepared dsDNA/GCE biosensor was washed in the PB for 5 s, and the recordings of CV and EIS were obtained in 1 mmol L^{-1} $[Fe(CN)_6]^{4-/3-}$ in the PB.

3.2 Hydroxyl radicals generated on the BDDE

The BDDE in the form of a plate, which was used for the generation of hydroxyl radicals causing oxidative dsDNA damage, was positioned in the measurement setup (see Fig. 1). The geometric active electrode area was defined by the Viton gasket, which has a round hole with a diameter of 0.6 cm (an active area of 0.28 cm^2). Firstly, the BBDE was activated using anodic oxidation in acidic medium (0.5 mol L^{-1} H_2SO_4) by inserting decomposition potential of background electrolyte (+2.4 V). Then, the surface of the prepared dsDNA/GCE biosensor (disconnected from the potentiostat) was placed in a parallel way close to the BDDE surface directly against each other (distance 3 mm) (see Fig. 1). Hydroxyl radicals were generated by the galvanostatic electrolysis on the BDDE in the PB and they migrated in the solution to the dsDNA/GCE biosensor. The current density is an important factor which corresponds to the ratio between the applied current and the area of the working electrode [21]. The different current densities (5–50 mA cm^{-2}) were examined during different periods of time. The BDDE area used and the current densities of 5, 10, and 50 mA cm^{-2} applied provided the resulting currents 1.41, 2.83, and 14.13 mA, respectively. The concentration profile of hydroxyl radicals during they generation is a function of the distance from the

electrode surface [5] because the very high reactivity of hydroxyl radicals results in their very short half-life (about 10^{-10} s), which explains why their concentration is generally very low [9]. After the interaction of the dsDNA/GCE biosensor with hydroxyl radicals, oxidative dsDNA damage was evaluated using the comprehensive electrochemical biosensing approach (detection techniques: SWV, CV, and EIS).

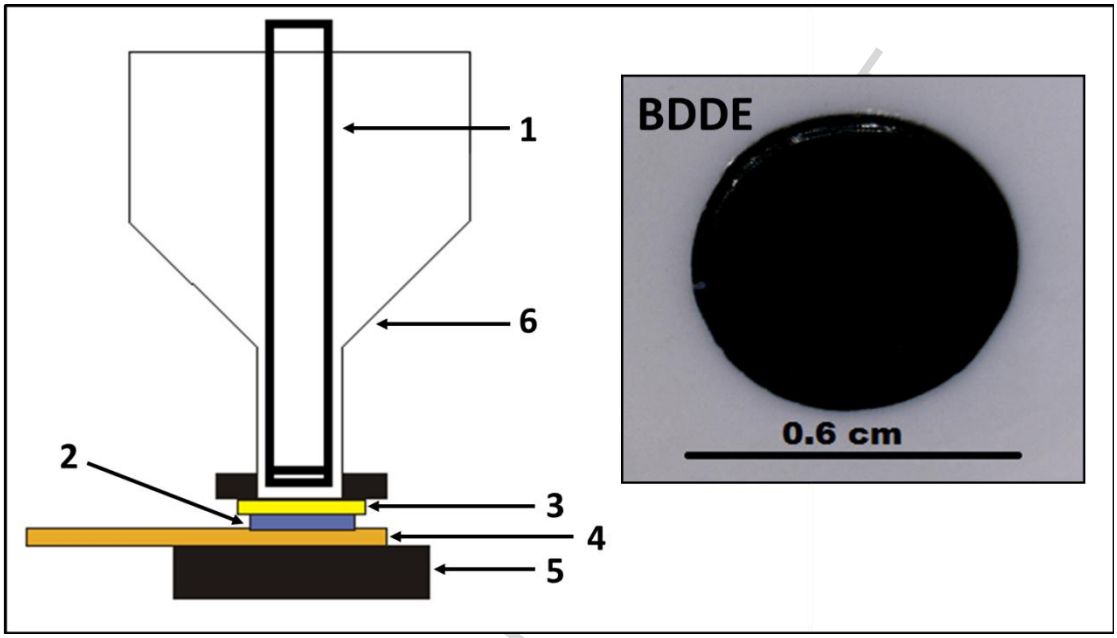

Fig. 1. The detailed scheme of the boron-doped diamond electrode (BDDE) used in our laboratory for the generation of hydroxyl radicals causing dsDNA damage at the dsDNA/GCE biosensor. On the left side the glass cell with the clamped BDDE: (1) the dsDNA/GCE biosensor, (2) the BDDE plate, (3) the Viton gasket, (4) the Cu plate (contact), (5) the insulating pad, and (6) the glass cell. On the right side the photo of the BDDE plate bounded by the Viton gasket with a diameter of 0.6 cm.

3.2.1 Investigation using square-wave voltammetry

SWV is a sensitive voltammetric technique allowing the use of relatively fast scan rate to detect the specific oxidation responses of dsDNA bases [16]. At the dsDNA/GCE biosensor, the changes in the intensity of the oxidation signals of dsDNA bases before and after the interaction with hydroxyl radicals were monitored. Three oxidation signals of dsDNA bases were registered: p_G – the peak of guanosine, p_A – the peak of adenosine, p_{TC} – the peak of thymidine and cytidine [5,26]. These anodic voltammetric peaks were observed at potentials of 1.01 V (p_G), 1.30 V (p_A), and 1.56 V (p_{TC}), respectively. Only peaks of guanosine and adenosine were involved in further research applications of the prepared dsDNA/GCE biosensor.

Hydroxyl radicals were generated by galvanostatic electrolysis on the BDDE in the PB applying the current densities of 5, 10, and 50 mA cm^{-2} for various incubation times (t_{inc}) (0.5, 1, 2, 3, 4, and 5 min) in non-stirred solution. For each t_{inc}, the dsDNA/GCE biosensor was also applied in the pure PB as blank. The peak current of guanosine and adenosine decreased with the increasing time of generating hydroxyl radicals. The higher and more pronounced dsDNA damage was observed with the increasing current density applied because the increasing amount of hydroxyl radicals was consequently produced. Baseline-corrected SWV responses of the dsDNA bases at the dsDNA/GCE biosensor before and after the interaction with hydroxyl radicals generated on the BDDE for the current density of 10 mA cm^{-2} are shown in Fig. 2A. The relative biosensor responses (for guanosine) for the current densities of 5, 10, and 50 mA cm^{-2} are shown in Fig. 2B. The fast and steep decrease in the relative biosensor response was observed for the current density of 50 mA cm^{-2}. During 1 min, the peak current of guanosine and adenosine dropped to minimum, and, then, the changes were much slower. For example, at the t_{inc} of 3 min, the relative biosensor responses decreased to about 38% (for p_G) and 44% (for p_A; data not shown) for the current density of 5 mA cm^{-2}, to about 27% (for p_G) and 35% (for p_A) for the current density of 10 mA cm^{-2}, and to about 3% (for p_G) and 2% (for p_A; data not shown) for the current density of 50 mA cm^{-2}.

After oxidative dsDNA damage by hydroxyl radicals (short-lived radicals oxidize the DNA bases and deoxyribose, which leads to the release of the bases and to the interruption of the phosphodiester bonds [8]), the formation of 8-oxoguanosine and 8-oxoadenosine was observed in other studies [5,11,27]. The mechanism of guanosine and adenosine transformation after the attack by hydroxyl radicals is interpreted in detail in literature [28,29]. In our case, oxidation products of dsDNA bases were not observed because they were probably immediately further oxidized by generated hydroxyl radicals, too.

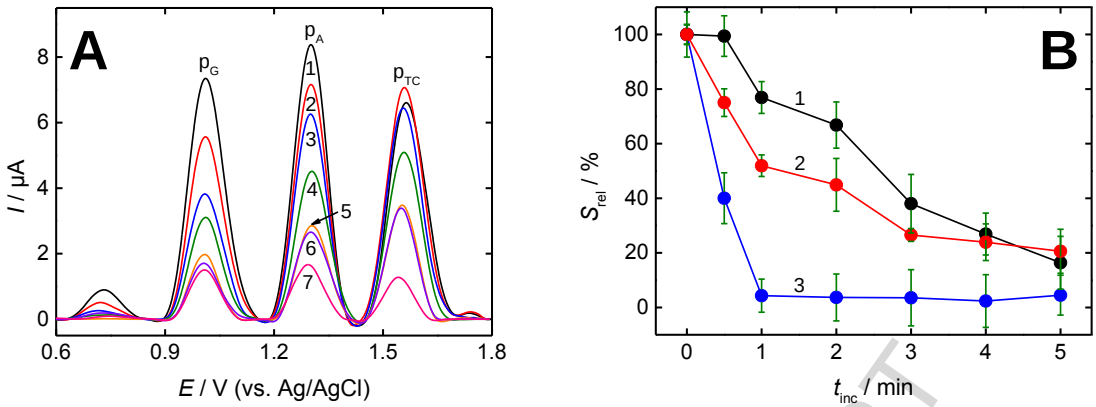

Fig. 2. (A) Baseline-corrected SWV responses of dsDNA bases at the dsDNA/GCE biosensor recorded in the PB before and after the interaction with hydroxyl radicals generated on the BDDE with the applied current density of 10 mA cm^{-2}. The dsDNA/GCE biosensor was immersed into solution containing hydroxyl radicals for the incubation time (t_{inc}) (min): 0 (1), 0.5 (2), 1 (3), 2 (4), 3 (5), 4 (6), and 5 (7). Oxidation signals: p_G – the peak of guanosine, p_A – the peak of adenosine, p_{TC} – the peak of thymidine and cytidine. (B) The corresponding relative biosensor responses (S_{rel}) evaluated using the guanosine peak plotted vs. the t_{inc} (0.5–5 min). Three different current densities were examined (mA cm^{-2}): 5 (1), 10 (2), and 50 (3). The error bars are constructed for the significance level of 0.05 (n = 3).

3.2.2 Investigation using cyclic voltammetry and electrochemical impedance spectroscopy

These methods use the redox-active indicator $[Fe(CN)_6]^{4-/3-}$, which indicates the presence of DNA layer on the electrode surface on the principle of electrostatic repulsion by the negatively charged DNA backbone [30,31]. They are used to detect survived portion of DNA and for simple electrochemical and electrical characterization of the electrode surface [3,16]. The measurement using CV and EIS lasts a longer time than SWV. The heights of the anodic ($I_{p,a}$) and cathodic ($I_{p,c}$) peaks of $[Fe(CN)_6]^{4-/3-}$ were measured by CV, and the charge transfer resistance (R_{CT}) was measured by EIS before and after the interaction of the dsDNA/GCE biosensor with hydroxyl radicals.

The dsDNA/GCE biosensor was incubated for various times (0.5, 1, 3, 5, 10, and 30 min) in the solution containing hydroxyl radicals generated by galvanostatic electrolysis on the BDDE with the current densities of 5, 10, and 50 mA cm^{-2} applied in the non-stirred PB. For each t_{inc}, the dsDNA/GCE biosensor was also applied in the pure PB as blank. The relative biosensor responses were evaluated from the changes of $I_{p,a}$, $I_{p,c}$, and R_{CT}. Both methods showed noticeable changes in the values of $I_{p,a}$, $I_{p,c}$, and R_{CT} for the lowest current density (5 mA cm^{-2}) (data not shown).

For CV, the relative biosensor responses (calculated from the values of $I_{p,a}$ and $I_{p,c}$) increased with the increasing t_{inc} for the current density of 10 mA cm^{-2} (data not shown). After 3 min incubation (data not shown), there was a very small increase in the relative

biosensor responses, and, for 30 min incubation (data not shown), the increase was to about 450% (for $I_{p,a}$) and 200% (for $I_{p,c}$). This behavior indicated the formation of a more compact molecular film on the GCE surface (probably caused by the interruption of the phosphodiester bonds in dsDNA [8] resulting in a denser coverage of the electrode surface; of course, also the oxidation of nucleobases occurred here (see Section 3.2.1), however, its influence is not detectable using these indirect methods – CV and EIS) than in the case of the originally adsorbed dsDNA. The electrode surface was thus more blocked to the molecules of $[Fe(CN)_6]^{4-/3-}$. For the higher current density of 50 mA cm^{-2} (see Fig. 3A and 3B), the situation was different. Firstly, the relative biosensor responses increased during the first 3 min of incubation (interruption of the phosphodiester bonds in dsDNA). For longer t_{inc}, the relative biosensor responses decreased (to about 60% (for $I_{p,a}$) and 80% (for $I_{p,c}$) for 30 min) as degraded dsDNA was released from the GCE surface, which resulted in a less blocking of the electrode surface to the molecules of $[Fe(CN)_6]^{4-/3-}$.

The relative biosensor response (calculated from the R_{CT} values measured by EIS) increased with the increasing t_{inc} for the current density of 10 mA cm^{-2} (data not shown). After 5 min incubation (data not shown), there was a very small increase in the relative biosensor response, and, for 30 min incubation (data now shown), the increase was to about 350%. The increase of the value of R_{CT} indicated smaller conductivity and a higher blocking of the GCE surface. For the higher current density of 50 mA cm^{-2} (see Fig. 3C and 3D), the relative biosensor response increased over 100% at the t_{inc} of 1 and 3 min (interruption of the phosphodiester bonds in dsDNA), however, it decreased with the increasing t_{inc} (to about 30% for 30 min) as degraded dsDNA fell down from the GCE surface (interruption of the phosphodiester bonds occurred [8], resulting in the destabilization of the electrostatic attraction between the negatively charged sugar–phosphate DNA backbone and the positively charged GCE surface). Therefore, the electrode surface had higher conductivity and was more accessible for the molecules of $[Fe(CN)_6]^{4-/3-}$.

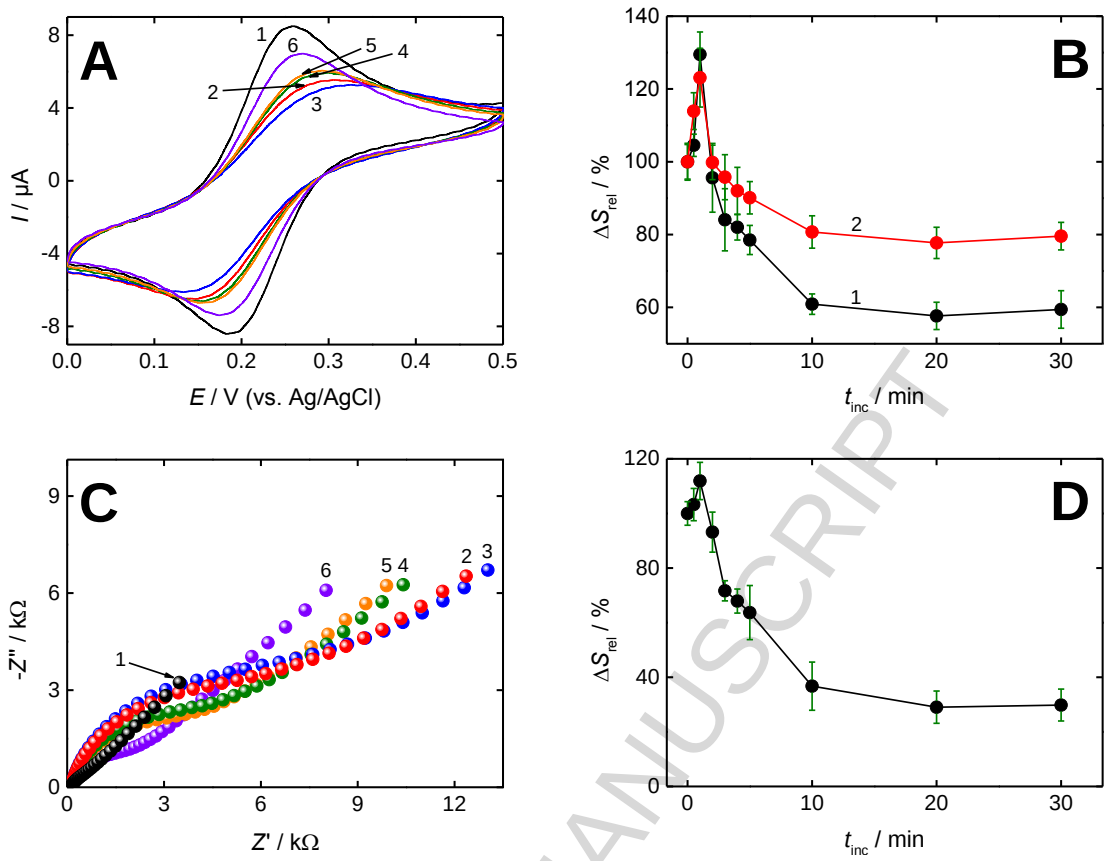

Fig. 3. (A) Cyclic voltammograms of 1 mmol L^{-1} $[Fe(CN)_6]^{4-/3-}$ in the PB recorded at the bare GCE (1) and at the dsDNA/GCE biosensor exposed to hydroxyl radicals (generated on the BDDE at the current density of 50 mA cm^{-2}) for the incubation time (t_{inc}) (min): 0 (2), 1 (3), 3 (4), 5 (5), and 30 (6). (B) The corresponding relative biosensor responses (ΔS_{rel}) evaluated using the anodic (1) and cathodic (2) peaks of $[Fe(CN)_6]^{4-/3-}$ plotted vs. the t_{inc} (0.5–30 min). (C) Nyquist plots recorded in the presence of 1 mmol L^{-1} $[Fe(CN)_6]^{4-/3-}$ in the PB at the bare GCE (1) and at the dsDNA/GCE biosensor exposed to hydroxyl radicals (generated on the BDDE at the current density of 50 mA cm^{-2}) for the t_{inc} (min): 0 (2), 1 (3), 3 (4), 5 (5), and 30 (6). (D) The corresponding ΔS_{rel} evaluated using the charge transfer resistance of $[Fe(CN)_6]^{4-/3-}$ plotted vs. the t_{inc} (0.5–30 min). For both (B) and (D): the error bars are constructed for the significance level of 0.05 (n = 3).

3.3 Hydroxyl radicals generated by the Fenton's reaction

There are many papers about the Fenton's reaction which provide suitable reaction conditions and concentrations of the Fenton's reagents [6,7,9,13]. For our experiments, optimum molar ratio of Fe(II):EDTA:H_2O_2 for running the Fenton's reaction was found. Hydroxyl radicals were formed after mixing Fe(II):EDTA:H_2O_2 (5:5:50 mmol L^{-1}) in the molar ratio of 1:1:10. The solution with the Fenton's reagents was filled up to 10 mL with the 0.1 mol L^{-1} acetate buffer of pH 4.7. The lower concentrations of the Fenton's reagents were not effective and thus not used. The Fenton's reaction mixture was prepared freshly before each measurement.

3.3.1 Investigation using square-wave voltammetry

Damage to DNA bases was confirmed by a decrease in electrochemical oxidation currents after the interaction with hydroxyl radicals generated by the Fenton's reaction. The prepared dsDNA/GCE biosensor was immersed into the freshly prepared Fenton's mixture for various t_{inc} (0.5, 1, 3, 5, 10, and 30 min) in non-stirred solution. For each t_{inc}, the dsDNA/GCE biosensor was also applied in the solution of Fe(II):EDTA (5:5 mmol L^{-1}) in the 0.1 mol L^{-1} acetate buffer of pH 4.7 as blank. SW voltammograms were recorded in the pure PB. Three oxidation signals of dsDNA bases (p_G, p_A, and p_{TC}) were registered. The peak current of guanosine and adenosine decreased with the increasing t_{inc} in the Fenton's mixture which generated hydroxyl radicals. Baseline-corrected SWV responses of the dsDNA bases at the dsDNA/GCE before and after the interaction with hydroxyl radicals are shown in Fig. 4A. The corresponding relative biosensor responses (for guanosine and adenosine) are shown in Fig. 4B. They decreased to about 49% (for p_G) and 28% (for p_A) for 10 min incubation. For 30 min incubation, they decreased to about 45% (for p_G) and 0.3% (for p_A), but the peak current of thymidine and cytidine (p_{TC}) increased. This can be caused by quenching the Fenton's reaction in a longer reaction time. The remaining free Fe(II), which did not react yet, interacted further with dsDNA (auto-oxidation reaction; see Section 3.4).

The results obtained at the dsDNA/GCE biosensor within the interaction with hydroxyl radicals generated by the Fenton's reaction are similar to those obtained within the interaction with hydroxyl radicals generated on the BDDE when the lower current densities were applied. Nevertheless, the dsDNA damage by the Fenton's reaction is not as pronounced as the dsDNA damage by hydroxyl radicals generated on the BDDE (see Fig. 2).

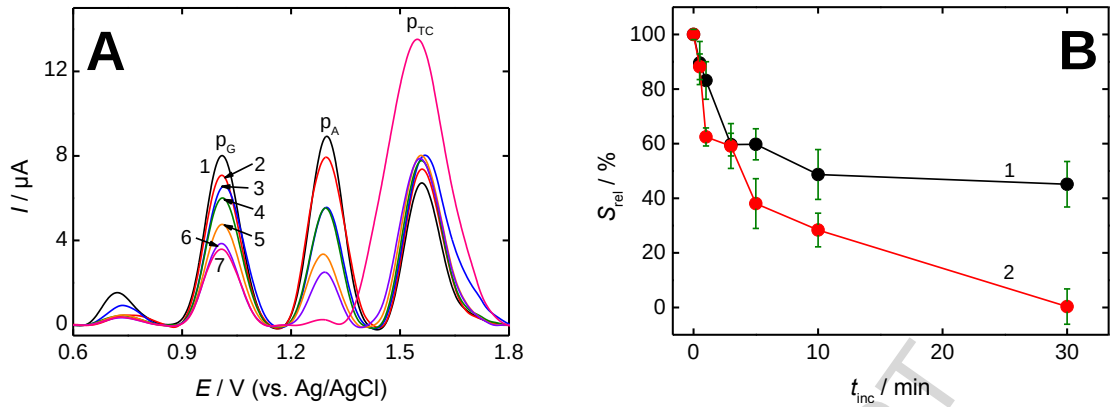

Fig. 4. (A) Baseline-corrected SWV responses of dsDNA bases at the dsDNA/GCE biosensor recorded in the PB before and after the interaction with hydroxyl radicals generated by the Fenton's reaction. The dsDNA/GCE biosensor was immersed into solution containing hydroxyl radicals for the incubation time (t_{inc}) (min): 0 (1), 0.5 (2), 1 (3), 3 (4), 5 (5), 10 (6), and 30 (7). Oxidation signals: p_G – the peak of guanosine, p_A – the peak of adenosine, p_{TC} – the peak of thymidine and cytidine. (B) The corresponding relative biosensor responses (S_{rel}) evaluated using the guanosine (1) and adenosine (2) peaks plotted vs. the t_{inc} (0.5–30 min). The error bars are constructed for the significance level of 0.05 (n = 3).

3.3.2 Investigation using cyclic voltammetry and electrochemical impedance spectroscopy

The time, for which the dsDNA/GCE biosensor was immersed into the non-stirred solution containing hydroxyl radicals generated by the Fenton's reaction, varied from 0.5 to 10 min. For each t_{inc}, the dsDNA/GCE biosensor was also applied in the solution of Fe(II):EDTA (5:5 mmol L^{-1}) in the 0.1 mol L^{-1} acetate buffer of pH 4.7 as blank. The changes in the values of $I_{p,a}$ and $I_{p,c}$ using CV and R_{CT} using EIS in time were measured in the presence of 1 mmol L^{-1} $[Fe(CN)_6]^{4-/3-}$ in the PB, and the relative biosensor responses were evaluated.

Cyclic voltammograms recorded at the dsDNA/GCE before and after the interaction with hydroxyl radicals generated by the Fenton's reaction are depicted in Fig. 5A. The relative biosensor responses (calculated from the values of $I_{p,a}$ and $I_{p,c}$) increased with the increasing t_{inc} (see Fig. 5B) to about 148% (for $I_{p,a}$) and 136% (for $I_{p,c}$) for 1 min incubation, to about 320% (for $I_{p,a}$) and 220% (for $I_{p,c}$) for 5 min incubation, and to about 540% (for $I_{p,a}$) and 290% (for $I_{p,c}$) for 10 min incubation. This behavior is very similar to the one observed within the initial stage (during the first 3 min of incubation) of the interaction with hydroxyl radicals generated on the BDDE (see Fig. 3B), indicating the formation of the more compact molecular film on the GCE surface after the interruption of the phosphodiester bonds in dsDNA [8]. On the other hand, no subsequent decrease in the relative biosensor responses (as shown in Fig. 3B) was registered here (see Fig. 5B). This is in accordance with the conclusion

in Section 3.3.1 that the dsDNA damage by the Fenton's reaction is not as pronounced as the dsDNA damage by hydroxyl radicals generated on the BDDE.

Nyquist plots recorded at the dsDNA/GCE before and after the interaction with hydroxyl radicals generated by the Fenton's reaction are depicted in Fig. 5C. The relative biosensor response (calculated from the R_{CT} values) increased with the increasing t_{inc} (see Fig. 5D) to about 139% for 1 min incubation, to about 300% for 5 min incubation, and to about 440% for 10 min incubation. The conductivity of the GCE surface decreased with the increasing extent of oxidative dsDNA damage. The longer t_{inc} was applied, the more the GCE surface was blocked. The compact molecular film was expanded in time, and, therefore, the R_{CT} values increased.

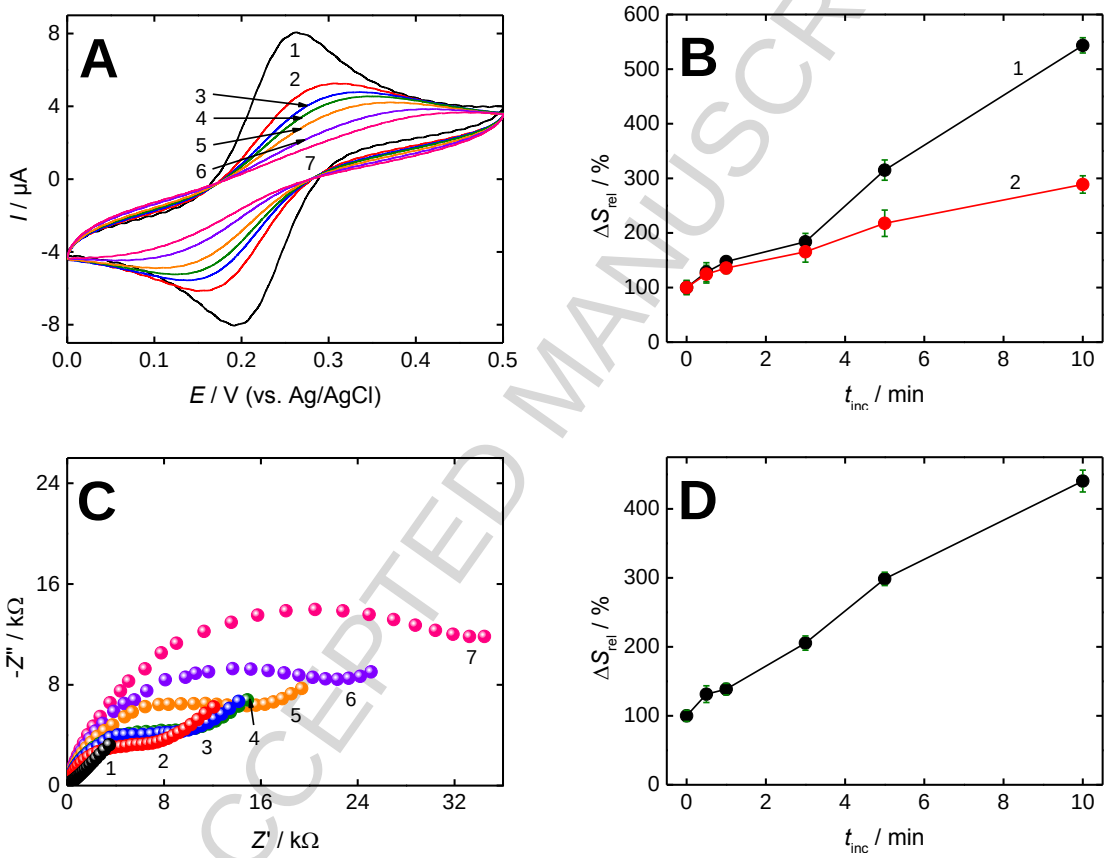

Fig. 5. (A) Cyclic voltammograms of 1 mmol L^{-1} $[Fe(CN)_6]^{4-/3-}$ in the PB recorded at the bare GCE (1) and the dsDNA/GCE biosensor exposed to hydroxyl radicals (generated by the Fenton's reaction) for the incubation time (t_{inc}) (min): 0 (2), 0.5 (3), 1 (4), 3 (5), 5 (6), and 10 (7). (B) The corresponding relative biosensor responses (ΔS_{rel}) evaluated using the anodic (1) and cathodic (2) peaks of $[Fe(CN)_6]^{4-/3-}$ plotted vs. the t_{inc} (0.5–10 min). (C) Nyquist plots recorded in the presence of 1 mmol L^{-1} $[Fe(CN)_6]^{4-/3-}$ in the PB at the bare GCE (1) and at the dsDNA/GCE biosensor exposed to hydroxyl radicals (generated by the Fenton's reaction) for the t_{inc} (min): 0 (2), 0.5 (3), 1 (4), 3 (5), 5 (6), and 10 (7). (D) The corresponding ΔS_{rel} evaluated using the charge transfer resistance of $[Fe(CN)_6]^{4-/3-}$ plotted vs. the t_{inc} (0.5–10 min). For both (B) and (D): the error bars are constructed for the significance level of 0.05 (n = 3).

3.4 Investigation of the auto-oxidation from Fe(II) to Fe(III)

The changes in the intensity of the oxidation signals of dsDNA bases before and after the interaction in solution of Fe(II) ions in the acetate buffer of pH 4.7 were monitored using SWV. Firstly, the dsDNA/GCE biosensor was immersed into solution containing Fe(II) (c = 100 μmol L^{-1}) for the t_{inc} ranging from 0.5 to 10 min (see Fig. 6A). For each t_{inc}, the dsDNA/GCE biosensor was also applied in the 0.1 mol L^{-1} acetate buffer of pH 4.7 as blank. The peak current of guanosine and adenosine decreased with the increasing t_{inc} (see Fig. 6B). The peak current of guanosine decreased to about 33% for 10 min incubation, and the peak current of adenosine decreased to 0% for 5 min incubation. The oxidation signal at potential of 1.55 V increased from 6 μA to 100 μA after incubation in solution of Fe(II), and its position is similar to the position of the thymidine and cytidine peak (p_{TC}).

Afterwards, SW voltammograms were recorded after 1 min incubation of the dsDNA/GCE biosensor in solutions where the concentration of Fe(II) (c_{Fe}) varied from 1 to 1000 μmol L^{-1} (see Fig. 6C). The peak currents of guanosine and adenosine decreased with the increasing c_{Fe} (see Fig. 6D) to about 63% (for p_G) and 42% (for p_A) for the c_{Fe} of 10 μmol L^{-1}, to about 47% (for p_G) for the c_{Fe} of 1000 μmol L^{-1}, and to 0% (for p_A) for the c_{Fe} of 500–1000 μmol L^{-1}. The oxidation signal at potential of 1.55 V increased from 6 μA to 80 μA after incubation in solution of Fe(II).

The oxidation signals of guanosine and adenosine decreased with the increasing t_{inc} and c_{Fe}. The auto-oxidation from Fe(II) to Fe(III) caused oxidative dsDNA damage (of a higher extent than that caused by the Fenton's reaction; see Section 3.3), but the overall mechanism of this dsDNA cleavage reaction is still unclear and under debate. The hydroxyl radical formation is probably promoted by the superoxide radical formation [32], and, moreover, free Fe(II) ions (not complexed with EDTA like they were in the Fenton's reaction mixture) are capable of binding to DNA [23] (see Section 1.3), thus inducing more serious dsDNA damage, since the hydroxyl radicals are formed in the intimate proximity of the dsDNA nucleobases. The increased oxidation signal at 1.55 V (see Fig. 6A and 6C) can be attributed to the electrochemical oxidation of products formed by opening the imidazole rings of purine nucleobases (guanine and adenine) as described in [28,29]. The supposed products (2,6-diamino-5-formamido-4-hydroxypyrimidine and 4,6-diamino-5-formamidopyrimidine [29]) are structurally similar to pyrimidine nucleobases (thymine and cytosine) which are oxidized at a very similar potential (peak p_{TC} at 1.56 V; see Fig. 2A). The overlapping of these peaks can be connected with the mentioned structural similarity.

For indirect methods (CV and EIS), the changes in the values of $I_{p,a}$, $I_{p,c}$, and R_{CT} were small even for the highest c_{Fe} (1000 μmol L^{-1}) for 10 min incubation (data not shown). The interruption of the phosphodiester bonds and the strand break formation (time progressive loss of the deeply degraded DNA from the biosensor surface) were not confirmed, as only very

small signal changes were observed. This is in good agreement with the fact that Fe(II) ions (having a high affinity to the nitrogenous bases of DNA [24]) are forming complexes with the nucleobases, and, therefore, hydroxyl radicals originating from the auto-oxidation of Fe(II) are preferentially attacking the nucleobases – such type of oxidative dsDNA damage is detectable using SWV, but not detectable using CV and EIS (see Section 3.2.2). Thus, these methods are not sensitive enough for the detection of DNA damage caused by the auto-oxidation from Fe(II) to Fe(III).

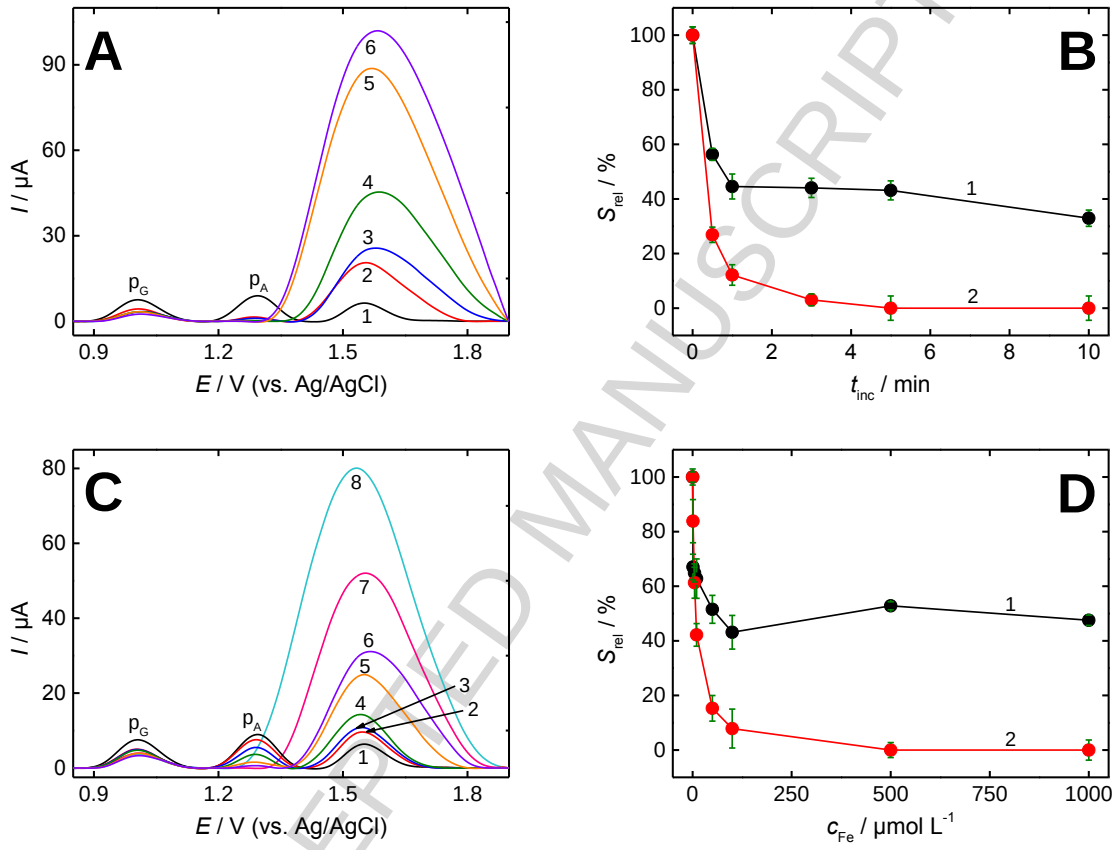

Fig. 6. (A) Baseline-corrected SWV responses of dsDNA bases at the dsDNA/GCE biosensor recorded in the PB before and after the interaction with hydroxyl radicals generated by the auto-oxidation of 100 µmol L^{-1} Fe(II) in the acetate buffer of pH 4.7. The dsDNA/GCE biosensor was immersed into solution containing hydroxyl radicals for the incubation time (t_{inc}) (min): 0 (1), 0.5 (2), 1 (3), 3 (4), 5 (5), and 10 (6). (B) The corresponding relative biosensor responses (S_{rel}) evaluated using the guanosine (1) and adenosine (2) peaks plotted vs. the t_{inc} (0.5–30 min). (C) Baseline-corrected SWV responses of dsDNA bases at the dsDNA/GCE biosensor recorded in the PB before and after the interaction with hydroxyl radicals generated by the auto-oxidation of Fe(II) in the acetate buffer of pH 4.7 for 1 min. The dsDNA/GCE biosensor was immersed into solution containing hydroxyl radicals generated by the auto-oxidation of Fe(II) of the concentration (c_{Fe}) (µmol L^{-1}): 0 (1), 1 (2), 5 (3), 10 (4), 50 (5), 100 (6), 500 (7), and 1000 (8). (D) The corresponding S_{rel} evaluated using the guanosine (1) and adenosine (2) peaks plotted vs. the c_{Fe} in the concentration range from 1 to 1000 µmol L^{-1}. Oxidation signals: p_G – the peak of guanosine, p_A – the peak of adenosine. For both (B) and (D): the error bars are constructed for the significance level of 0.05 (n = 3).

4. Conclusions

A simple electrochemical DNA biosensor (dsDNA/GCE biosensor) based on a glassy carbon electrode (GCE) and low molecular weight double-stranded DNA (dsDNA) was prepared and employed in the comprehensive electrochemical biosensing approach (introduced by Labuda *et al.* [3,16]) representing a novel model for *in vitro* classification of potentially genotoxic chemicals. By the help of this tool, dsDNA damage induced by hydroxyl radicals was investigated and its extent was evaluated. The obtained results demonstrate that the proposed electrochemical methods are likely to find further application in DNA damage studies (*e.g.*, in elucidation of the mechanism by which DNA is oxidatively damaged by various reactive radical species).

Damage to dsDNA was induced by exposing the dsDNA/GCE biosensor to hydroxyl radicals generated either electrochemically (on the surface of a boron-doped diamond electrode (BDDE)) or chemically (via the Fenton's reaction or the auto-oxidation of Fe(II)). The extent of dsDNA damage depends on the current density applied to the BDDE, on the suitable molar ratio of Fe(II):EDTA:H_2O_2 for running the Fenton's reaction, on the concentration of Fe(II) undergoing the auto-oxidation, and on the reaction time for which the hydroxyl radicals were in contact with dsDNA. In all experiments performed, dsDNA was attacked and oxidized by hydroxyl radicals, which resulted in the oxidation of nucleobases and the interruption of phosphodiester bonds. Consequently, fragments of damaged dsDNA fell down from the GCE surface, or formed a more compact film and thus blocked the GCE surface more intensely.

Acknowledgement

This research was carried out in the framework of the Specific University Research (SVV 2017). A.H. thanks the Grant Agency of the Charles University (Project GAUK 430214/2014/B-CH/PrF), and J.B. and V.V. thank the Grant Agency of the Czech Republic (Project P206/12/G151) for the financial support.

References

[1] A.A. Ensafi, N. Kazemnadi, M. Amini, B. Rezaei, Impedimetric DNA-biosensor for the study of dopamine induces DNA damage and investigation of inhibitory and repair effects of some antioxidants, Bioelectrochemistry, 104 (2015) 71–78.

[2] A.A. Ensafi, M. Amini, B. Rezaei, Assessment of genotoxicity of catecholics using impedimetric DNA-biosensor, Biosens. Bioelectron., 53 (2014) 43–50.

[3] L. Hlavata, K. Benikova, V. Vyskocil, J. Labuda, Evaluation of damage to DNA induced by UV-C radiation and chemical agents using electrochemical biosensor based on low molecular weight DNA and screen-printed carbon electrode, Electrochim. Acta, 71 (2012) 134–139.

[4] X.L. Wang, R. Chen, L. Sun, Z.Y. Yu, Study on the antioxidant capacities of four antioxidants based on oxidizing guanine in a composite membrane, Int. J. Electrochem. Sci., 9 (2014) 6834–6842.

[5] S.C.B. Oliveira, A.M. Oliveira-Brett, In situ DNA oxidative damage by electrochemically generated hydroxyl free radicals on a boron-doped diamond electrode, Langmuir, 28 (2012) 4896–4901.

[6] J.J. Zhang, B. Wang, Y.F. Li, W.L. Jia, H. Cui, H.S. Wang, Electrochemical study on DNA damage based on the direct oxidation of 8-hydroxydeoxyguanosine at an electrochemically modified glassy carbon electrode, Electroanalysis, 20 (2008) 1684–1689.

[7] M.F. Barroso, C. Delerue-Matos, M. Oliveira, Electrochemical evaluation of total antioxidant capacity of beverages using a purine-biosensor, Food Chem., 132 (2012) 1055–1062.

[8] H.Y. Xiong, Y. Wang, X.H. Zhang, Y. Ye, S.F. Wang, Evaluation of antioxidative capacity via measurement of the damage of DNA using an electrochemical biosensor and an ionic liquid solvent, Microchim. Acta, 176 (2012) 479–484.

[9] I. Gualandi, D. Tonelli, A new electrochemical sensor for OH radicals detection, Talanta, 115 (2013) 779–786.

[10] H.Y. Xiong, Y. Chen, X.H. Zhang, H.S. Gu, S.F. Wang, An electrochemical biosensor for the rapid detection of DNA damage induced by xanthine oxidase-catalyzed Fenton reaction, Sens. Actuators B-Chem., 181 (2013) 85–91.

[11] S.C.B. Oliveira, A.M. Oliveira-Brett, Boron doped diamond electrode pre-treatments effect on the electrochemical oxidation of dsDNA, DNA bases, nucleotides, homopolynucleotides and biomarker 8-oxoguanine, J. Electroanal. Chem., 648 (2010) 60–66.

[12] A. Baumann, W. Lohmann, S. Jahn, U. Karst, On-line electrochemistry/electrospray ionization mass spectrometry (EC/ESI-MS) for the generation and identification of nucleotide oxidation products, Electroanalysis, 22 (2010) 286–292.

[13] A.H. Kamel, F.T.C. Moreira, C. Delerue-Matos, M.G.F. Sales, Electrochemical determination of antioxidant capacities in flavored waters by guanine and adenine biosensors, Biosens. Bioelectron., 24 (2008) 591–599.

[14] A. Hajkova, J. Barek, V. Vyskocil, Voltammetric determination of 2-aminofluoren-9-one and investigation of its interaction with DNA on a glassy carbon electrode, Electroanalysis, 27 (2015) 101–110.

[15] V. Vyskocil, A. Hajkova, Novel electrochemical DNA biosensors as tools for investigation and detection of DNA damage, in: F.-M. Matysik (Ed.), Trends in Bioelectroanalysis, Springer International Publishing, Cham, 2016, pp. 203–221.

[16] G. Ziyatdinova, J. Labuda, Complex electrochemical and impedimetric evaluation of DNA damage by using DNA biosensor based on a carbon screen-printed electrode, Anal. Methods, 3 (2011) 2777–2782.

[17] S.C.B. Oliveira, A.M. Oliveira-Brett, Voltammetric and electrochemical impedance spectroscopy characterization of a cathodic and anodic pre-treated boron doped diamond electrode, Electrochim. Acta, 55 (2010) 4599–4605.

[18] E. Hmani, Y. Samet, R. Abdelhedi, Electrochemical degradation of auramine-O dye at boron-doped diamond and lead dioxide electrodes, Diam. Relat. Mater., 30 (2012) 1–8.

[19] Y. Samet, L. Agengui, R. Abdelhedi, Electrochemical degradation of chlorpyrifos pesticide in aqueous solutions by anodic oxidation at boron-doped diamond electrodes, Chem. Eng. J., 161 (2010) 167–172.

[20] J. Barek, J. Fischer, T. Navratil, K. Peckova, B. Yosypchuk, J. Zima, Nontraditional electrode materials in environmental analysis of biologically active organic compounds, Electroanalysis, 19 (2007) 2003–2014.

[21] N. Rabaaoui, M.E.K. Saad, Y. Moussaoui, M.S. Allagui, A. Bedoui, E. Elaloui, Anodic oxidation of o-nitrophenol on BDD electrode: Variable effects and mechanisms of degradation, J. Hazard. Mater., 250 (2013) 447–453.

[22] M. Mazloum-Ardakani, E. Salehpour, M.M. Heidari, A. Zomorodipour, The effect of pomegranate juice as a natural antioxidant to prevent DNA damages is detectable by application of electrochemical methods, Sci. Iran., 20 (2013) 566–570.

[23] S.S. Babkina, N.A. Ulakhovich, Complexing of heavy metals with DNA and new bioaffinity method of their determination based on amperometric DNA-based biosensor, Anal. Chem., 77 (2005) 5678–5685.

[24] A.A. Ouameur, H. Arakawa, R. Ahmad, M. Naoui, H.A. Tajmir-Riahi, A comparative study of Fe(II) and Fe(III) interactions with DNA duplex: Major and minor grooves bindings, DNA Cell Biol., 24 (2005) 394–401.

[25] L.A. Loeb, E.A. James, A.M. Waltersdorph, S.J. Klebanoff, Mutagenesis by the autooxidation of iron with isolated DNA, Proc. Natl. Acad. Sci. USA, 85 (1988) 3918–3922.

[26] A.M. Oliveira-Brett, J.A.P. Piedade, L.A. Silva, V.C. Diculescu, Voltammetric determination of all DNA nucleotides, Anal. Biochem., 332 (2004) 321–329.

[27] V.C. Diculescu, A.M.C. Paquim, A.M.O. Brett, Electrochemical DNA sensors for detection of DNA damage, Sensors, 5 (2005) 377–393.

[28] L.D. Mello, S. Hernandez, G. Marrazza, M. Mascini, L.T. Kubota, Investigations of the antioxidant properties of plant extracts using a DNA-electrochemical biosensor, Biosens. Bioelectron., 21 (2006) 1374–1382.

[29] J. Cadet, T. Douki, D. Gasparutto, J.L. Ravanat, Radiation-induced damage to cellular DNA: Measurement and biological role, Radiat. Phys. Chem., 72 (2005) 293–299.

[30] M. Ozsoz, Electrochemical DNA biosensors, Taylor and Francis Group, Boca Raton, 2012.

[31] M. Fojta, A. Danhel, L. Havran, V. Vyskocil, Recent progress in electrochemical sensors and assays for DNA damage and repair, Trends Anal. Chem., 79 (2016) 160–167.

[32] K. Keyer, J.A. Imlay, Superoxide accelerates DNA damage by elevating free-iron levels, Proc. Natl. Acad. Sci. USA, 93 (1996) 13635–13640.

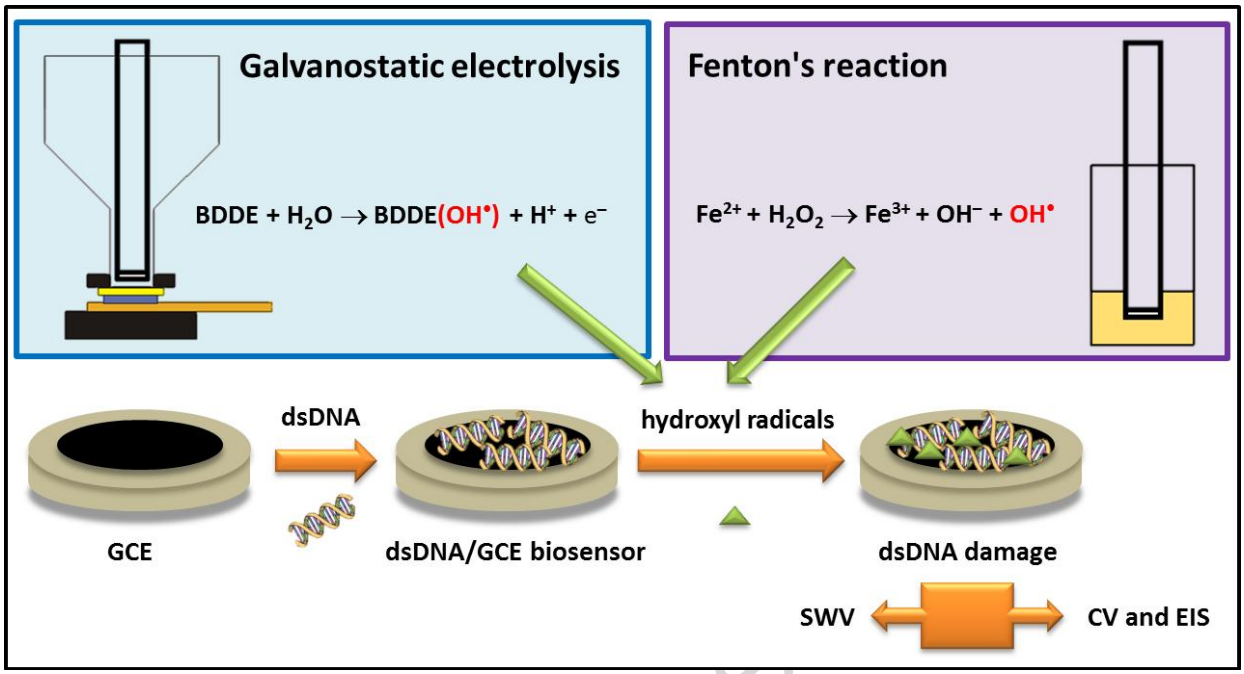

Graphical Abstract

Highlights

- Oxidative DNA damage was detected after interaction with hydroxyl radicals.
- Electrochemically (vs. chemically) generated radicals caused more pronounced damage.
- Radicals were active even in 3 mm distance from their source (boron-doped diamond electrode).
- DNA damage by auto-oxidation of Fe(II) was detected electrochemically for the first time.
- Fe(II) ions caused time- and concentration-dependent DNA damage.